Weak N^* Production and SU(6)*

C. H. ALBRIGHT AND L. S. LIU
Department of Physics, Northwestern University, Evanston, Illinois
(Received 25 June 1965)

A phenomenological study is made of the weak N^* production process by displaying the matrix element in terms of eight form factors. Simple functional dependences are adopted for these form factors, and analytical expressions for the cross sections are given in detail. A numerical analysis is carried out to investigate the effectiveness of each form factor. Three models are proposed for this process: One assumes the dominance of a single form factor, another incorporates information obtained from N^* photoproduction, and the third employs the $SU(6)$ relations of Bég and Pais. All three models are compatible with the present experimental information, but the one derived from the $SU(6)$ theory is the most encouraging.

I. INTRODUCTION

FIVE years have passed since Schwartz and Pontecorvo independently proposed using neutrinos from the decay of intense, well-collimated beams of high-energy pions to probe the weak interactions.[1] Since then, experiments at both Brookhaven[2] and CERN[3] have provided much information about the weak interactions, to wit: The separate identities of the muon and electron neutrinos, ν_μ and ν_e; the absolute conservation of leptons; the apparent absence of neutral lepton currents; and the nonexistence of intermediate bosons with mass less than 2 BeV. Even more information about the weak interactions will be gained when the antineutrino experiments now in progress at CERN are analyzed.

Quite aside from the information gained about the weak interactions, it has recently become apparent that high-energy neutrinos also serve as a useful probe of the strong interactions. For example, on the basis of $SU(3)$ unitary symmetry,[4] one should expect to see in addition to the ordinary "elastic" process,

$$\nu_l+n\rightarrow p+l, \tag{1.1}$$

the competing process

$$\nu_l+N\rightarrow N^*+l \tag{1.2}$$

involving the direct production of the 3-3 pion-nucleon isobar $N^*(1238)$.

The most detailed information about reaction (1.2) at present comes from the CERN high-energy neutrino experiment and is supplied by the CERN heavy-liquid bubble-chamber group.[5] They find that the number of elastic and inelastic neutrino events are comparable. Moreover, below 4 BeV, most of the inelastic events involve single-pion production, i.e.,

$$\nu_l+N\rightarrow l+N+\pi. \tag{1.3}$$

Their analysis of the invariant mass spectrum and the charge/neutral pion ratio demonstrated in fact that a large fraction of these single-pion events proceed via the production of an N^* and its subsequent decay: $N^*\rightarrow N+\pi$. Thus the importance of process (1.2) has been confirmed.

According to the usual $SU(3)$ assignments, process (1.1) represents an octet-octet transition, while process (1.2) represents an octet-decuplet transition. As such the two processes are not simply related. However, if one adopts the $SU(6)$ symmetry scheme[6] according to which the baryon $\frac{1}{2}^+$ octet and the baryon $\frac{3}{2}^+$ decuplet are both members of the same $SU(6)$ supermultiplet, **56**, the two reactions become intimately connected.

As a probe of the strong interactions, the high-energy neutrinos are thus able to make some critical tests of the higher symmetry schemes recently proposed. In this respect, the neutrino experiments play much the same role as the high-energy electron-scattering experiments. Neutrinos have the added advantage, however, that they are able to probe the strong interactions via both the vector- and axial-vector-type couplings by virtue of the dual-parity nature of the weak interactions.

In this paper, we present a detailed phenomenological study of the weak N^* production process, (1.2), and its $SU(3)$-symmetric counterpart,

$$\nu_l+N\rightarrow Y_1^*+l, \tag{1.4}$$

where the $Y_1^*(1385)$ is the $I=1$ member of the decuplet. The role of the neutrino as a probe of the strong interactions is exploited fully in that the transition matrix for (1.2) or (1.4) is written in terms of eight form factors which are functions only of the momentum-transfer variable. The effectiveness of each of these form factors in contributing to the total cross section is then investigated. We also present the detailed predictions for the N^* and Y_1^* production processes derived

* Supported in part by the National Science Foundation.

[1] M. Schwartz, Phys. Rev. Letters **4**, 306 (1960); B. Pontecorvo, Zh. Eksperim. i Teor. Fiz. **37**, 1751 (1959) [English transl.: Soviet Phys.—JETP **10**, 1236 (1960)].

[2] G. Danby *et al.*, Phys. Rev. Letters **9**, 36 (1962); G. Danby *et al.*, *ibid.* **10**, 260 (1963); R. Burns *et al.*, *ibid.* **15**, 42 (1965).

[3] M. M. Block *et al.*, Phys. Letters **12**, 281 (1964); J. K. Beinlein *et al.*, *ibid.* **13**, 80 (1964); G. Bernardini *et al.*, *ibid.* **13**, 86 (1964).

[4] M. Gell-Mann, California Institute of Technology Synchrotron Laboratory Report CTSL-20, 1961 (unpublished); Y. Ne'eman, Nucl. Phys. **26**, 222 (1961).

[5] Block *et al.*, see Ref. 3.

[6] F. Gürsey and L. A. Radicati, Phys. Rev. Letters **13**, 173 (1964); A. Pais, *ibid.* **13**, 175 (1964); B. Sakita, Phys. Rev. **136**, B1756 (1964).

from the elastic reaction on the basis of the $SU(6)$ symmetry scheme. Although the experimental uncertainties are large, the theoretical results are encouraging. Some of the results obtained in our study were briefly reported in two letters.[7,8] In another paper to be published,[9] we shall report on the cross-section results derived from the relativistic generalizations of $SU(6)$ and compare them with those found in this paper in the nonrelativistic SU (6) theory.

Several authors[10] have also made a phenomenological study of the N^* process from a somewhat different point of view. Weaver *et al.* chose the simplified case with only one form factor present, while Zheleznykh singled out two form factors. Berman and Veltman, on the other hand, selected several of the form factors and fixed their strength according to the conserved-vector-current and almost-conserved-axial-vector-current hypotheses. Kim has also made an analysis similar to the latter two authors.

Prior to the suggestion of the eightfold way[4] by Gell-Mann and Ne'eman, it was natural to focus one's attention on process (1.3) instead of (1.2). The peripheral model with one-pion exchange or W-meson exchange was considered by a number of authors for this single-pion production process.[11] In this approach, the effect of the N^* is inserted to enhance the appropriate intermediate state in a dispersion-theoretical or static-model calculation. Since this analysis involves a number of invariant-scattering amplitudes which are functions of two variables, it is very complex and the interpretation somewhat uncertain. Their approach is to be contrasted with ours, where the N^* is produced directly.

The outline of our work is the following. The N-N^* transition matrix element is written in terms of eight form factors in Sec. II, while III contains the differential cross section and its low-momentum-transfer limit. The effectiveness of the various form factors is investigated in Sec. IV for two different momentum-transfer dependences. Section V contains the predictions of $SU(6)$ and the conserved-vector-current hypothesis, and VI summarizes the findings of our phenomenological approach. The rather lengthy formulas are recorded in the Appendices.

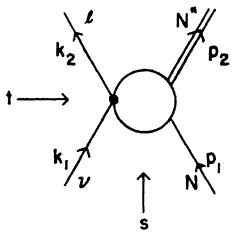

FIG. 1. N^* production by neutrinos: notation.

II. WEAK N^* PRODUCTION MATRIX ELEMENT

The generic weak N^* production process,

$$\nu_l+N\rightarrow N^*+l, \tag{2.1}$$

is illustrated in Fig. 1, where a point interaction is assumed for the leptons. We denote by $k_1(\omega_1)$, $p_1(E_1)$, $k_2(\omega_2)$, and $p_2(E_2)$ the four-momenta (energy) of the neutrino, nucleon of mass M_1, lepton of mass m_l, and isobar of mass M_2, respectively.[12] The invariants s and t are defined by the equations

$$\begin{aligned} s&=-(p_1+k_1)^2=-(p_2+k_2)^2,\\ t&=-(p_2-p_1)^2=-(k_1-k_2)^2=-q^2. \end{aligned} \tag{2.2}$$

The spin-$\frac{3}{2}$ isobar is described by a spinor-vectorial field $\psi_\mu(p_2)$ in the Rarita-Schwinger formalism[13] with the subsidiary conditions

$$\gamma_\mu\psi_\mu=0,$$

and

$$p_{2\mu}\psi_\mu=0, \tag{2.3}$$

employed to project out the spin-$\frac{1}{2}$ components. The four independent spin states are given by

$$\begin{aligned} \psi_\mu^{(\frac{3}{2})}&=e_\mu^{(1)}u_+,\\ \psi_\mu^{(\frac{1}{2})}&=\sqrt{\tfrac{2}{3}}\,e_\mu^{(0)}u_++\sqrt{\tfrac{1}{3}}\,e_\mu^{(1)}u_-,\\ \psi_\mu^{(-\frac{1}{2})}&=\sqrt{\tfrac{1}{3}}\,e_\mu^{(-1)}u_++\sqrt{\tfrac{2}{3}}\,e_\mu^{(0)}u_-,\\ \psi_\mu^{(-\frac{3}{2})}&=e_\mu^{(-1)}u_-, \end{aligned} \tag{2.4}$$

where

$$\begin{aligned} e_\mu^{(1)}&=-\frac{1}{\sqrt{2}}(1,i,0;0),\\ e_\mu^{(0)}&=(0,0,(E_2/M_2);i(p_2/M_2)),\\ e_\mu^{(-1)}&=\frac{1}{\sqrt{2}}(1,-i,0;0), \end{aligned} \tag{2.5}$$

are the polarization vectors of the vectorial field. The z axis has been selected as the quantization axis which is defined by the direction of the N^* momentum. The Dirac spinors u_+ and u_- with spin up and spin down, respectively, are normalized according to $\bar{u}_iu_j=\delta_{ij}$. The adjoints of the unit four-vectors $e_\mu^{(\lambda)}=(\mathbf{e}^{(\lambda)};ie_0^{(\lambda)})$ are

[7] C. H. Albright and L. S. Liu, Phys. Rev. Letters **13**, 673 (1964).

[8] C. H. Albright and L. S. Liu, Phys. Rev. Letters **14**, 324; 532(E) (1965).

[9] C. H. Albright and L. S. Liu, Phys. Rev. (to be published).

[10] D. L. Weaver, H. S. Song, C. L. Hammer, and R. H. Good, Jr., Nuovo Cimento **35**, 150 (1965); I. M. Zheleznykh, Phys. Letters **11**, 251 (1964); S. M. Berman and M. Veltman, Nuovo Cimento **38**, 993 (1965); C. W. Kim, Nuovo Cimento **37**, 142 (1965).

[11] J. S. Bell and S. M. Berman, Nuovo Cimento **25**, 404 (1962); N. Cabibbo and G. Da Prato, *ibid.* **25**, 611 (1962); N. Dombey, Phys. Rev. **127**, 653 (1962); P. Dennery, *ibid.* **127**, 664 (1962); Nguyen Van-Hieu, Zh. Eksperim. i Teor. Fiz. **43**, 1296 (1962) [English transl.: Soviet Phys.—JETP **16**, 920 (1963)]; A. Fujii and E. Celeghini, Nuovo Cimento **28**, 90 (1963); G. R. Henry, J. Løvseth, and J. D. Walecka, *ibid.* **36**, 509 (1965).

[12] We use the Minkowski metric, and all γ matrices are taken to be Hermitian.

[13] W. Rarita and J. Schwinger, Phys. Rev. **60**, 61 (1940); S. Kusaka, *ibid.* **60**, 61 (1940).

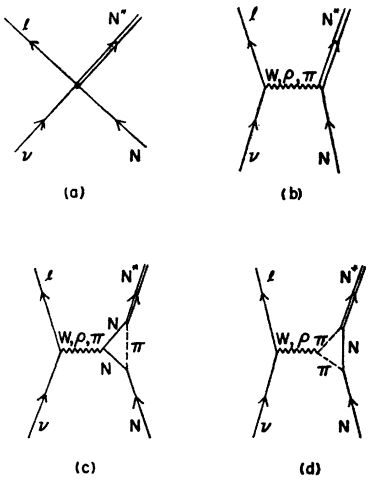

FIG. 2. Feynman diagrams for N^* production.

given by

$$\bar{e}_\mu{}^{(\lambda)}=(\mathbf{e}^{(\lambda)*};ie_0{}^{(\lambda)}), \tag{2.6}$$

where the asterisk indicates complex conjugation. For an arbitrary polarization state of N^*, it is convenient to write

$$\psi_\mu=(\psi,i\psi_0)=g_\mu u_+ + f_\mu u_- \equiv h_\mu u; \tag{2.7}$$

then the Pauli adjoint field is given by

$$\bar{\psi}_\mu=(\bar{\psi},i\bar{\psi}_0)\equiv\bar{h}_\mu\bar{u},$$

where the adjoint of h_μ is defined in the same manner as that for $e_\mu{}^{(\lambda)}$. With $\bar{g}\cdot g+\bar{f}\cdot f=1$, ψ_μ is normalized to unity.

The dynamics of the N^* production process (2.1) is all contained in the N-N^* transition vertex which can be described in terms of eight form factors under the assumption of a local $V-A$ lepton current. In particular, the production matrix element can be written as

$$\mathfrak{M}=\frac{G}{\sqrt{2}}\langle N^*|J_\mu|N\rangle\bar{u}_l\gamma_\mu(1+\gamma_5)u_\nu, \tag{2.8}$$

where the transition vertex is given by[14]

$$\begin{aligned}\langle N^*|J_\mu|N\rangle=&\bar{\psi}_\lambda[\delta_{\lambda\mu}(F_1{}^A+F_1{}^V\gamma_5)\\&+ip_{1\lambda}\gamma_\mu(F_2{}^A+F_2{}^V\gamma_5)/(M_1+M_2)\\&+p_{1\lambda}(p_1+p_2)_\mu(F_3{}^A+F_3{}^V\gamma_5)/(M_1+M_2)^2\\&+p_{1\lambda}(p_1-p_2)_\mu(F_4{}^A+F_4{}^V\gamma_5)/(M_1+M_2)^2]u_N\end{aligned} \tag{2.9}$$

for the $J^P=\frac{3}{2}+$ N^* isobar. This form is convenient for calculation; an alternative form for the vector contribution is

$$\begin{aligned}\langle N^*|J_\mu{}^V|N\rangle=&\bar{\psi}_\lambda[\delta_{\lambda\mu}H_1{}^V+ip_{1\lambda}\gamma_\mu H_2{}^V/(M_1+M_2)\\&+ip_{1\lambda}\sigma_{\mu\alpha}(p_1-p_2)_\alpha H_3{}^V/(M_1+M_2)^2\\&+p_{1\lambda}(p_1-p_2)_\mu H_4{}^V/(M_1+M_2)^2]\gamma_5 u_N,\end{aligned} \tag{2.10}$$

where the two sets of vector form factors are related by

$$\begin{aligned}&F_1{}^V=H_1{}^V,\\&F_2{}^V=H_2{}^V+[(M_2-M_1)/(M_1+M_2)]H_3{}^V,\\&F_3{}^V=-H_3{}^V,\ F_4{}^V=H_4{}^V.\end{aligned} \tag{2.11}$$

The form factors are functions only of the momentum transfer t, and are all relatively real if time-reversal invariance holds.[15]

In Fig. 2 we have singled out some Feynman diagrams which may make significant contributions to these form factors. A direct 4-fermion interaction is pictured in Fig. 2(a); representative particle exchange diagrams are shown in Figs. 2(b), (c), and (d) where the diagrams in (c) and (d) exhibit anomalous threshold behavior in the t channel. Table I spells out explicitly to which form factors $F_i{}^{V,A}$ the various diagrams of Fig. 2 contribute.

If one imposes the conserved-vector-current (CVC) hypothesis[16] for this octet-decuplet transition, only three vector form factors are linearly independent, i.e.,

$$\begin{aligned}&(M_1+M_2)^2(F_1{}^V+F_2{}^V)\\&\qquad+(M_2{}^2-M_1{}^2)F_3{}^V-tF_4{}^V=0.\end{aligned} \tag{2.12}$$

However, we shall not impose this restriction at the outset.

We conclude this section by elaborating the charge channels of process (2.1):

$$\nu_l+n\rightarrow N^{*+}+l^-, \tag{2.13a}$$

$$\nu_l+p\rightarrow N^{*++}+l^-. \tag{2.13b}$$

By analogy with the "elastic" process, $\nu_l+n\rightarrow p+l^-$, we denote the coupling constant for reaction (2.13a) simply by G, where $GM_p{}^2=1.02\times10^{-5}$; for reaction (2.13b) the appropriate coupling constant is then $\sqrt{3}G$ under the assumption that the weak current transforms like an isospin vector operator.

TABLE I. Form factors receiving contributions from the diagrams of Fig. 2 as indicated by an X.

Feynman diagram of Fig. 2	Particle exchanged	$F_1{}^A$	$F_1{}^V$	$F_2{}^A$	$F_2{}^V$	$F_3{}^A$	$F_3{}^V$	$F_4{}^A$	$F_4{}^V$
a	⋯	X	X	X	X	X	X	X	X
b	W	X	X	X	X	X	X	X	X
	ρ		X		X		X		X
	π						X		
c	W			X	X	X	X	X	X
	ρ				X		X		X
	π					X		X	
d	W					X	X	X	X
	ρ						X		X

[14] Note that here we have selected the mass $M=M_1+M_2$ to render all the form factors dimensionless. In Refs. 7 and 8 we used $M=M_1$. The new choice seems to be a more natural one as will be seen in Sec. III, when we discuss the differential cross section at low-momentum transfer.

[15] The analytic expressions derived allow complex form factors, but all are taken to be real in our later numerical work.

[16] S. Gerschtein and J. Zeldovich, Zh. Eksperim. i Teor. Fiz. **29**, 689 (1955) [English transl.: Soviet Phys.—JETP **2**, 576 (1956)]; R. P. Feynman and M. Gell-Mann, Phys. Rev. **109**, 193 (1958).

The reactions corresponding to (2.13) for N^* production by antineutrinos are:

$$\bar{\nu}_l+p\rightarrow N^{*0}+l^+, \tag{2.14a}$$

$$\bar{\nu}_l+n\rightarrow N^{*-}+l^+. \tag{2.14b}$$

Here the appropriate coupling constants are G and $\sqrt{3}G$, respectively, for (2.14a) and (2.14b). The matrix element for (2.14a) is then given by

$$\mathfrak{M}'=\frac{G}{\sqrt{2}}\langle N^{*0}|J_\mu^\star|p\rangle\bar{v}_\nu\gamma_\mu(1+\gamma_5)v_l, \tag{2.15}$$

in terms of the negative-energy Dirac spinors for the antileptons, where

$$\begin{aligned} J_\mu^\star&=-J_\mu^\dagger, \quad \mu=1,2,3\\ &=\ J_\mu^\dagger, \quad \mu=4 \end{aligned} \tag{2.16}$$

and J_μ is the Heisenberg current operator which raises the z component of isospin by one unit while $J_\mu^\dagger$ lowers I_z by one unit. If we now invoke the $\Delta I=1$ rule, i.e.,

$$RJ_\mu R^{-1}=-J_\mu^\star, \tag{2.17}$$

in terms of a rotation about the y axis by π radians, Eq. (2.15) can be rewritten as

$$\mathfrak{M}'=\frac{G}{\sqrt{2}}\langle N^{*+}|J_\mu|n\rangle\bar{v}_\nu\gamma_\mu(1+\gamma_5)v_l, \tag{2.18}$$

where here the $N-N^*$ transition vertex is just that given by Eq. (2.9).

III. INVARIANT DIFFERENTIAL CROSS SECTION FOR N^* PRODUCTION

The invariant differential cross section[17] for V^* production is given by

$$\frac{d\sigma}{dt}=\frac{1}{2\pi}\frac{T}{(s-M_1^2)^2}, \tag{3.1}$$

where

$$T=M_1M_2m_1\omega_1\sum|\mathfrak{M}|^2, \tag{3.2}$$

and summation over the ν, N, N^*, and l spins are implied. In order to carry out the spin summations, it is convenient to sum first over the ν, N, and l spins and write

$$\begin{aligned} \tfrac{1}{2}\sum_{\nu,N,l}|\mathfrak{M}^{(\lambda)}|^2&=\tfrac{1}{2}\sum_{\nu,N,l}\mathfrak{M}^{(\lambda)}\mathfrak{M}^{(\lambda)\dagger}\\ &=-(m_1\omega_1)^{-1}M_{\mu\sigma}{}^{(\lambda)}L_{\mu\sigma}, \end{aligned} \tag{3.3}$$

where

$$\begin{aligned} L_{\mu\sigma}&=L_{\mu\sigma}{}^S+L_{\mu\sigma}{}^A,\\ L_{\mu\sigma}{}^S&=k_{2\mu}k_{1\sigma}+k_{1\mu}k_{2\sigma}-k_1\cdot k_2\delta_{\mu\sigma},\\ L_{\mu\sigma}{}^A&=-\epsilon_{\mu\sigma\alpha\beta}k_{2\alpha}k_{1\beta}, \end{aligned}$$

and

$$M_{\mu\sigma}{}^{(\lambda)}=\tfrac{1}{2}G^2\sum_N\langle N^{*(\lambda)}|J_\mu|N\rangle\langle N^{*(\lambda)}|J_\sigma|N\rangle^\star.$$

Here the adjoint matrix element is found to be

$$\begin{aligned} \langle N^*|J_\sigma|N\rangle^\star=\bar{u}_N[&-\delta_{\rho\sigma}(F_1{}^{A^*}-F_1{}^{V^*}\gamma_5)\\ &-ip_{1\rho}\gamma_\sigma(F_2{}^{A^*}+F_2{}^{V^*}\gamma_5)/(M_1+M_2)\\ &-p_{1\rho}(p_1+p_2)_\sigma(F_3{}^{A^*}-F_3{}^{V^*}\gamma_5)/(M_1+M_2)^2\\ &-p_{1\rho}(p_1-p_2)_\sigma(F_4{}^{A^*}-F_4{}^{V^*}\gamma_5)/(M_1+M_2)^2]\psi_\rho. \end{aligned} \tag{3.4}$$

The summation over the N^* spin states may then be carried out with the help of the spin-$\frac{3}{2}$ projection operator

$$\begin{aligned} \sum_\lambda\psi_\mu{}^{(\lambda)}\bar{\psi}_\rho{}^{(\lambda)}=\Big\{&\delta_{\mu\rho}+\tfrac{2}{3}\frac{p_{2\mu}p_{2\rho}}{M_2{}^2}-\tfrac{1}{3}\gamma_\mu\gamma_\rho\\ &-\frac{i}{3M_2}(\gamma_\mu p_{2\rho}-\gamma_\rho p_{2\mu})\Big\}\frac{-i\gamma\cdot p_2+M_2}{2M_2}. \end{aligned} \tag{3.5}$$

After the spin sums are performed, it is apparent that T can be expressed in the following form:

$$T=\tfrac{4}{3}G^2\sum_{i=1}^{5}R_i(t)X_i(s,t), \tag{3.6}$$

where

$$\begin{aligned} X_1&=(p_2\cdot k_2)(p_1\cdot k_1)+(p_2\cdot k_1)(p_1\cdot k_2),\\ X_2&=(p_2\cdot k_2)(p_1\cdot k_1)-(p_2\cdot k_1)(p_1\cdot k_2),\\ X_3&=(p_2\cdot k_2)(p_2\cdot k_1),\\ X_4&=(p_1\cdot k_2)(p_1\cdot k_1),\\ X_5&=M_1M_2(k_1\cdot k_2). \end{aligned} \tag{3.7}$$

The $R_i(t)$ are functions only of t and are listed in Appendix B, where the X_i are also expressed explicitly in terms of s and t.

From the above grouping of terms, it is clear that only X_2 is antisymmetric under k_1, k_2 interchange; hence only $R_2(t)$ contains V-A interference terms which are generated by $M_{\mu\sigma}L_{\mu\sigma}{}^A$. The doubly-induced form factors $F_3{}^{V,A}$ and $F_4{}^{V,A}$, however, do not contribute to R_2 because of energy-momentum conservation and the presence of the antisymmetric tensor in $L_{\mu\sigma}{}^A$. Finally, we note that for the antineutrino processes (2.14), the V-A interference term reverses sign so R_2X_2 should be replaced by its negative with the other R_iX_i left unchanged.

Aside from the above general statements, little can be said about the behavior of the differential cross section until some assumptions are made for the functional t dependence of the eight form factors. However, for small four-momentum transfer, the invariant differential cross section depends only on the normaliza-

[17] The kinematics and the differential cross section in both center-of-mass and laboratory systems are elaborated in Appendix A.

TABLE II. High-energy cross-section behavior arising from each $F_i^{V,A}$ of Eq. (4.1) with $n=0$, 1, or 2. At large s, $\sigma(s)=(G^2/4\pi)|F_i^{V,A}(0)|^2\times$(appropriate entry in table).

Form factor	High-energy cross-section behavior $n=0$	$n=1$	$n=2$
F_1^A	$\frac{s^2}{18M_2^2}$	$\frac{b^2}{3M_2^2}\ln\left(\frac{s}{b}\right)$	$\frac{b}{9M_2^2}[(M_1+M_2)^2+\frac{1}{2}b]$
F_1^V	$\frac{s^2}{18M_2^2}$	$\frac{b^2}{3M_2^2}\ln\left(\frac{s}{b}\right)$	$\frac{b}{9M_2^2}[(M_2-M_1)^2+\frac{1}{2}b]$
F_2^A	$\frac{11s^3}{180M_2^2(M_1+M_2)^2}$	$\frac{2b^2s}{9M_2^2(M_1+M_2)^2}$	$\frac{b^3}{9M_2^2(M_1+M_2)^2}\left[1+\frac{M_1^2+M_2^2}{b}+\frac{(M_2^2-M_1^2)^2}{b^2}\right]$
F_2^V	$\frac{11s^3}{180M_2^2(M_1+M_2)^2}$	$\frac{2b^2s}{9M_2^2(M_1+M_2)^2}$	$\frac{b^3}{9M_2^2(M_1+M_2)^2}\left[1+\frac{M_1^2+M_2^2}{b}+\frac{(M_2^2-M_1^2)^2}{b^2}\right]$
F_3^A	$\frac{s^4}{60M_2^2(M_1+M_2)^4}$	$\frac{b^2s^2}{18M_2^2(M_1+M_2)^4}$	$\frac{b^4}{3M_2^2(M_1+M_2)^4}\ln\left(\frac{s}{b}\right)$
F_3^V	$\frac{s^4}{60M_2^2(M_1+M_2)^4}$	$\frac{b^2s^2}{18M_2^2(M_1+M_2)^4}$	$\frac{b^4}{3M_2^2(M_1+M_2)^4}\ln\left(\frac{s}{b}\right)$
F_4^A	$\frac{m_l^2s^3}{60M_2^2(M_1+M_2)^4}$	$\frac{m_l^2b^2s}{36M_2^2(M_1+M_2)^4}$	$\frac{m_l^2b^4}{12M_2^2(M_1+M_2)^4s}$
F_4^V	$\frac{m_l^2s^3}{60M_2^2(M_1+M_2)^4}$	$\frac{m_l^2b^2s}{36M_2^2(M_1+M_2)^4}$	$\frac{m_l^2b^4}{12M_2^2(M_1+M_2)^4s}$

tion of the form factors at $t\simeq 0$. In the limit $t\to 0^-$, it takes on the following form:

$$\frac{d\sigma}{dt}(0)\simeq\frac{G^2}{12\pi}\frac{s-M_2^2}{s-M_1^2}\left(\frac{M_1+M_2}{M_2}\right)^2\times\left\{|F_1^A|^2+2\frac{M_2-M_1}{M_1+M_2}\mathrm{Re}(F_1^AF_2^{A*}+F_1^AF_3^{A*})+\left(\frac{M_2-M_1}{M_1+M_2}\right)^2[|F_2^A|^2+|F_3^A|^2+|F_1^V|^2+|F_2^V|^2+2\,\mathrm{Re}(F_2^AF_3^{A*}+F_1^VF_2^{V*})]+2\left(\frac{M_2-M_1}{M_1+M_2}\right)^3\mathrm{Re}(F_1^VF_3^{V*}+F_2^VF_3^{V*})+\left(\frac{M_2-M_1}{M_1+M_2}\right)^4|F_3^V|^2\right\}. \quad (3.8)$$

Terms involving $[m_l/(M_1+M_2)]^2$ have been dropped; hence $F_4^{V,A}$ do not appear in the above equation since their coefficients are proportional to the lepton mass. The direct axial-vector term $|F_1^A|^2$ appears to be the most effective one for this limiting differential cross section. The other form factor combinations fall into several groups[18] according to powers of the mass difference, M_2-M_1. It would thus seem that the next leading contribution should result from the interference of F_2^A and F_3^A with F_1^A—at least at low-momentum transfer.

IV. PHENOMENOLOGICAL FORM FACTORS AND NUMERICAL RESULTS

We now turn our attention to a phenomenological study of the t dependence for the eight $N-N^*$ transition form factors. One salient feature for this study is that the high-energy behavior of the total cross section depends critically on the functional dependence of the $F_i^{V,A}(t)$. We shall use this as a guide for the selection of the phenomenological forms.

To calculate the total cross section, we have considered the following conventional t dependences:

$$F_i^{V,A}(t)=F_i^{V,A}(-q^2)=[F_i^{V,A}(0)]/[(1-t/b)^n], \quad (4.1)$$

where $n=0$, 1, and 2. For $n=0$, the form factors are structureless; for $n=1$, they have a simple pole dependence; while for $n=2$, they are analogous to the empirical ones appearing in elastic electron scattering from nucleons.[19] We have evaluated the asymptotic behavior of $\sigma(s)$ arising from the eight form factors individually with the above three t dependences of Eq. (4.1). The results are listed in Table II.

[18] This is a result of our selection of $M=M_1+M_2$ to render all form factors dimensionless, see Ref. 14.

[19] See, e.g., R. Hofstadter, F. Bumiller, and M. R. Yearian, Rev. Mod. Phys. 30, 482 (1958).

The structureless case, $n=0$, results in a highly divergent cross section arising from each of the eight form factors. This is clearly unacceptable. For the simple pole dependence, the direct form factors $F_1{}^{V,A}$ are weakly divergent while the others are more strongly divergent. With a small damping effect at large momentum transfer, this behavior is barely acceptable for the direct factors but still unacceptable for the other contributions. On the other hand, the Hofstadter-type dependence yields an acceptable asymptotic cross section for all form factors provided only slight modifications are made for $F_3{}^V$ and $F_3{}^A$. The differential cross section has been integrated analytically for the latter two cases, and the total cross section formulas are listed in Appendix C.

In Figs. 3 and 4, the numerical results are presented for the simple pole and Hofstadter cases, where the individual form factors have been taken one at a time. The cutoff parameter b is set equal to $(0.850\ \text{BeV})^2$ which is appropriate for the elastic reaction,[19,20] and all form factors have been normalized to unity. With this normalization, it is evident from Fig. 3 and Eq. (3.8) that the relative contributions fall into several groups with $F_1{}^A$ giving the leading one and in this sense being the most effective. One also notes that the asymptotic behavior of the total cross section given in Table II becomes apparent even for the moderate energy region included in Fig. 4.

The current experimental information for the weak N^* production process is supplied solely by the CERN heavy liquid bubble chamber group of Block *et al.*[3] Their results consist of total cross section measurements up to 6 BeV which are plotted in Fig. 5; in addition, they estimated an invariant differential cross section at low-momentum transfer given by

$$d\sigma/dq^2=(0.5\pm0.2)\times10^{-38}\ \text{cm}^2/(\text{BeV}/c)^2\ \text{per nucleon} \quad (4.2)$$

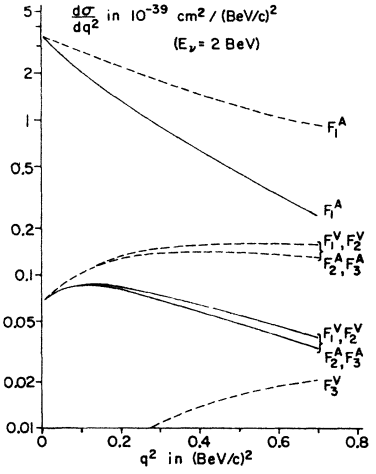

FIG. 3. Invariant differential cross section for the inelastic process $\nu_\mu+n\rightarrow N^{*+}+\mu^-$ for each form factor taken one at a time and normalized to unity with $\sqrt{b}=850$ MeV. The dashed curves refer to $n=1$ and the solid curves to $n=2$ in Eq. (4.1).

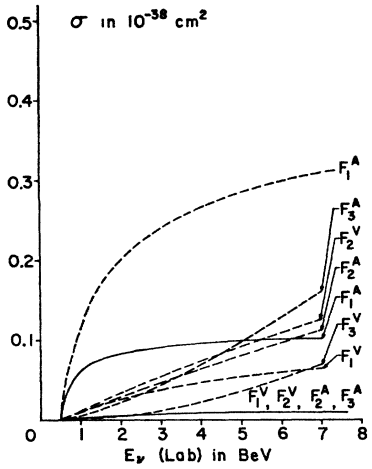

FIG. 4. Total cross section for $\nu_\mu+n\rightarrow N^{*+}+\mu^-$ corresponding to Fig. 3.

averaged over the momentum range $0\leq q^2\leq0.2$ $(\text{BeV}/c)^2$ and energy range $1.0\leq E_\nu\leq3.0$ BeV. To obtain the cross sections for the particular charge channel $\nu_\mu+n\rightarrow N^{*+}+\mu^-$, one must divide their results per nucleon by a factor of two.

Although the experimental uncertainties are rather large, several features are revealing. The information provided by the differential cross-section measurement at low-momentum transfer is valuable since it is independent of the q^2 structure of the individual form factors and depends only on their normalizations. The direct axial vector form factor $F_1{}^A$ by itself is able to accommodate the experimental range quoted in Eq. (4.2) with normalization near unity, unlike the other seven form factors. Moreover, $F_1{}^A$ yields a rapidly rising total cross section above threshold which is characteristic of the experimental histogram in Fig. 5. These results suggest that the simplest N^* production mechanism is through $F_1{}^A$ alone.

With this simplicity in mind, we have attempted to fit the total cross section data by adjusting the cutoff parameter b for the simple pole and Hofstadter cases of Eq. (4.1). The results are presented in Figs. 6 and 7.

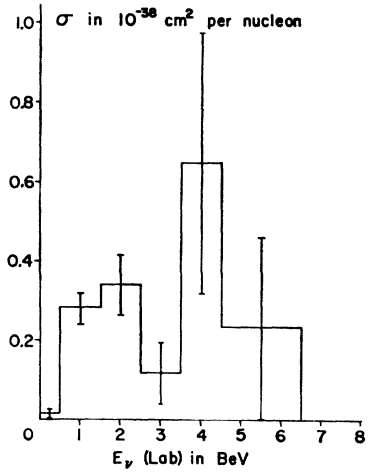

FIG. 5. Experimental cross section per nucleon for single-pion events as measured by the CERN group, see Ref. 5.

[20] Variation of the cutoff parameter b has a sizeable effect on the total cross section and the forward/backward ratio. This was previously reported in Ref. 7.

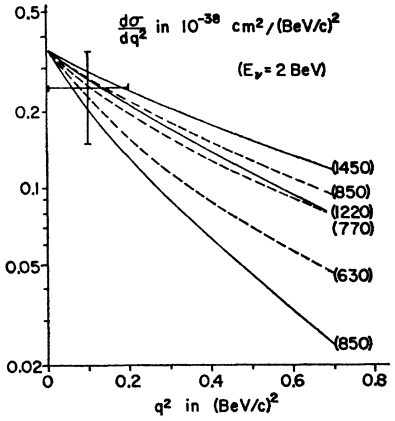

FIG. 6. Differential cross section for $\nu_\mu + n \to N^{*+} + \mu^-$ with pure F_1^A normalized to unity. Dashed curves refer to $n=1$, solid curves to $n=2$. The number in parentheses for each curve is equal to $\sqrt{b}$ in MeV. This convention is used hereafter.

For the $n=2$ case, a median value of (1.22 BeV)^2 for b provides a reasonable fit. On the other hand, a lower median value of (0.77 BeV)^2 provides a somewhat poorer fit for the $n=1$ case. This single form factor mechanism predicts an equal N^* production cross section by antineutrinos and is thus subject to a simple experimental test.

Perhaps a more reasonable mechanism is obtained by considering F_1^A together with some vector contribution. In particular, the CVC hypothesis relates the vector form factors for the weak $n \to N^{*+}$ process with those present in N^* photoproduction from nucleons. One finds the following relationship for the matrix elements:

$$\langle N^{*+}|J_\mu^V|n\rangle = \langle N^{*+}|J_\mu^{el}|p\rangle. \tag{4.3}$$

The N^* isobaric model has been used by Gourdin and Salin[21] to analyze the pion photoproduction process. In their notation, the electromagnetic vertex is given by

$$\langle N^{*+}|J_\mu^{el}|p\rangle = \bar{\psi}_\lambda[C_1\delta_{\lambda\mu}\gamma_5 - (C_2/m_\pi)ip_{1\lambda}\gamma_\mu\gamma_5]u_p, \tag{4.4}$$

where $C_1(0)$ and $C_2(0)$ are deduced to be 5.6 and 0.37, respectively. These numbers then imply that we take[14]

$$F_1^V(0)=5.6 \quad \text{and} \quad F_2^V(0)=-5.6 \tag{4.5}$$

for the $n \to N^{*+}$ process. Since their analysis indicates that both F_3^V and F_4^V are very small, Eq. (2.12) is satisfied.

In Figs. 8 and 9 we have plotted the differential and total cross sections using the vector form factors normalized according to Eqs. (4.5) and taking $F_1^A(0) = -0.87$ so as to yield a more nearly correct differential cross section at low-momentum transfer. The opposite sign of $F_1^A(0)$ is not considered since it leads to a decidedly worse fit to the total cross section near threshold. For the range of cutoff parameters included, a good fit is obtained with a median value of $b \approx$ (0.67 BeV)^2 for $n=2$. The simple-pole-type form factors, on the other hand lead to a very poor fit, and this case has not been plotted.

V. PREDICTIONS OF $SU(6)$ AND THE CVC HYPOTHESIS

In the last section, we have first investigated the effectiveness of the various form factors in contributing to the total cross section and then attempted to "fit" the experimental results in a rather *ad hoc* fashion by adjusting the normalizations and cutoff parameters. The recent development of the $SU(6)$ symmetry scheme, on the other hand, enables one to correlate the $n \to N^*$ inelastic and $n \to p$ "elastic" processes and hence to specify the $F_i^{V,A}(0)$. Here we present the results based on an analysis of the detailed predictions of $SU(6)$ and the CVC hypothesis for the form factors.

In the $SU(6)$ symmetry scheme,[6] the baryon $J^P=\frac{1}{2}^+$ octet and the baryon $\frac{3}{2}^+$ decuplet are conveniently assigned to the 56-dimensional irreducible representation since the spin–unitary-spin content is given by $\mathbf{56}=(2,8)+(4,10)$. The PS meson octet and the V meson nonet, on the other hand, can be placed in the adjoint representation, **35**, since $\mathbf{35}=(1,8)+(3,8)+(3,1)$. In the framework of $SU(6)$, Bég and Pais[22] have extended Cabibbo's original hypothesis[23] by making the assumption that the weak vector and axial vector currents of the hadrons transform like members of two different **35**'s. The effective matrix element for the semileptonic interaction

$$\nu_l + B_1 \to B_2 + l^- \tag{5.1}$$

can then be written in the low-frequency limit as

$$\langle B_2\mathbf{56}|\frac{G_V}{\sqrt{2}}J_\mu^V(\mathbf{35}) + \frac{G_A}{\sqrt{2}}J_\mu^A(\mathbf{35})|B_1\mathbf{56}\rangle L_\mu = 3B_{i\alpha,j\beta,k\gamma}^\dagger(p_2)B^{i\alpha,j\beta,r\rho}(p_1)C_{r\rho}{}^{k\gamma}(q), \tag{5.2}$$

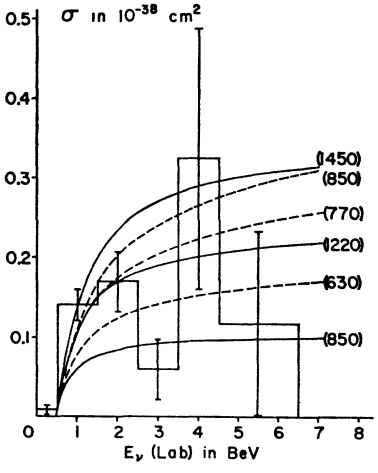

FIG. 7. Total cross section corresponding to Fig. 6.

[21] M. Gourdin and Ph. Salin, Nuovo Cimento **27**, 193, 309 (1963).

[22] M. A. B. Bég and A. Pais, Phys. Rev. Letters **14**, 51 (1965). Note that an error in the sign of the μ_W term of Eq. (2) has been corrected.

[23] N. Cabibbo, Phys. Rev. Letters **10**, 531 (1963).

where

$$C_{r\rho}{}^{k\gamma}(q)=\frac{G_V}{\sqrt{2}}[\delta_r{}^k(L_0)_\rho{}^\gamma-i\mu_W(\boldsymbol{\sigma}\cdot\mathbf{q}\times\mathbf{L}_\rho{}^\gamma)_r{}^k]+\tfrac{3}{5}\frac{G_A}{\sqrt{2}}(\boldsymbol{\sigma}\cdot\mathbf{L}_\rho{}^\gamma)_r{}^k, \quad (5.3)$$

$$\mu_W=\tfrac{3}{5}[\mu(p)-\mu(n)]\frac{1}{e}, \quad (5.4)$$

and $q=p_2-p_1$. The completely symmetric baryon tensor of the **56** in the rest frame can be reduced in terms of the spin and unitary spin tensors[24] according to

$$B^{i\alpha,i\beta,k\gamma}(0)=\chi^{ijk}d^{\alpha\beta\gamma}+\frac{1}{3\sqrt{2}}[(2\epsilon^{ij}\chi^k+\epsilon^{jk}\chi^i)\epsilon^{\alpha\beta\delta}b_\delta{}^\gamma+(\epsilon^{ij}\chi^k+2\epsilon^{ik}\chi^i)\epsilon^{\beta\gamma\delta}b_\delta{}^\alpha], \quad (5.5)$$

where the Latin indices take on the values 1, 2 and the Greek indices the values 1, 2, 3. The lepton four-vector matrix $L_\mu=(\mathbf{L},iL_0)$ is given by

$$L_\mu=\begin{pmatrix}0 & l_\mu\cos\theta & l_\mu\sin\theta\\ l_\mu{}^\dagger\cos\theta & 0 & 0\\ l_\mu{}^\dagger\sin\theta & 0 & 0\end{pmatrix}, \quad (5.6)$$

where

$$-il_\mu=\bar{u}_l(k_2)\gamma_\mu(1+\gamma_5)u_\nu(k_1), \quad (5.7)$$

and θ represents the Cabibbo angle, $\theta\approx 15°$.

An important consequence of this $SU(6)$ scheme lies in the fact that the octet-decuplet transitions can be related to the "elastic" octet-octet transitions since both $SU(3)$ baryon multiplets belong to the same $SU(6)$ supermultiplet. Thus one can make use of the parameters determined in the well-known $n\to p$ process ($G_VM_p{}^2=1.02\times10^{-5}$ and $G_A=1.2G_V$) to predict results for the other processes, e.g., $n\to N^{*+}$ and $p\to Y_1{}^{*0}$.

We consider first the inelastic reaction $n\tfrac{1}{2}\to N^{*+}\tfrac{1}{2}$, where the $\tfrac{1}{2}$ denotes the third component of spin. Here the appropriate tensor components are $b_3{}^2\chi^1$ for $n\tfrac{1}{2}$ while for N^{*+} we use $\sqrt{3}d^{112}=\sqrt{3}d^{121}=\sqrt{3}d^{211}$ with its spin $+\tfrac{1}{2}$ component denoted by $\sqrt{3}\chi^{112}=\sqrt{3}\chi^{121}=\sqrt{3}\chi^{211}$. We then have in the nonrelativistic limit

$$\mathfrak{M}_{\rm NR}(n\tfrac{1}{2}\to N^{*+}\tfrac{1}{2})=\langle N^{*+}\tfrac{1}{2}|\,(G_V/\sqrt{2})J_\mu{}^V+(G_A/\sqrt{2})J_\mu{}^A\,|n\tfrac{1}{2}\rangle L_\mu$$
$$=\frac{G_V}{\sqrt{2}}(\cos\theta)\frac{2\sqrt{2}}{3}\mu_W i(\mathbf{q}\times\mathbf{l})_3-\frac{G_A}{\sqrt{2}}(\cos\theta)\frac{2\sqrt{2}}{5}l_3. \quad (5.8)$$

This result is to be compared with the nonrelativistic limit of (2.9) which implies

$$\mathfrak{M}_{\rm NR}(n\tfrac{1}{2}\to N^{*+}\tfrac{1}{2})=\frac{G}{\sqrt{2}}\left\{\frac{1}{2\sqrt{6}\bar{M}}[F_1{}^V(0)-F_2{}^V(0)]\times(\mathbf{q}\times\mathbf{l})_3-\sqrt{\tfrac{2}{3}}iF_1{}^A(0)l_3\right\}, \quad (5.9)$$

where $\bar{M}$ is set equal to $(M_1+M_2)/2$. A straightforward identification leads to[14]

$$F_1{}^V(0)-F_2{}^V(0)=\frac{4\sqrt{3}}{5}\frac{\mu(p)-\mu(n)}{e/2\bar{M}}=7.5 \quad (5.10a)$$

and

$$F_1{}^A(0)=-\frac{2\sqrt{3}}{5}\frac{G_A}{G_V}=-0.83, \quad (5.10b)$$

with G set equal to $G_V\cos\theta$. The magnitude of $F_1{}^A(0)$ is determined uniquely with its phase fixed relative to $F_1{}^V(0)$. In the low-frequency limit with the baryon masses degenerate, no information is obtained about the remaining five induced form factors.

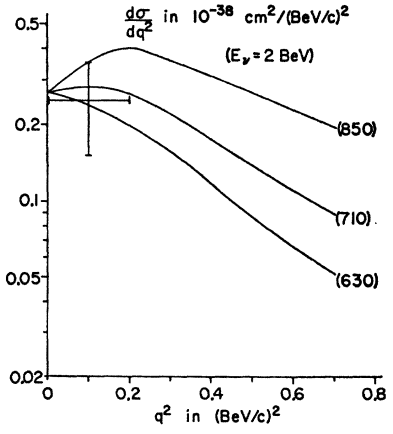

FIG. 8. Differential cross section for $\nu_\mu+n\to N^{*+}+\mu^-$ with $F_1{}^A(0)=-0.87$ and $F_1{}^V(0)$ and $F_2{}^V(0)$ derived from N^* photoproduction data. Only case $n=2$ is plotted.

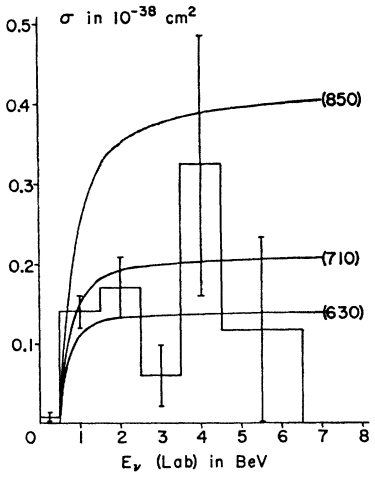

FIG. 9. Total cross section corresponding to Fig. 8.

[24] The notation for the spin and unitary spin tensors is given in M. A. B. Bég, B. W. Lee, and A. Pais, Phys. Rev. Letters 13, 514 (1964).

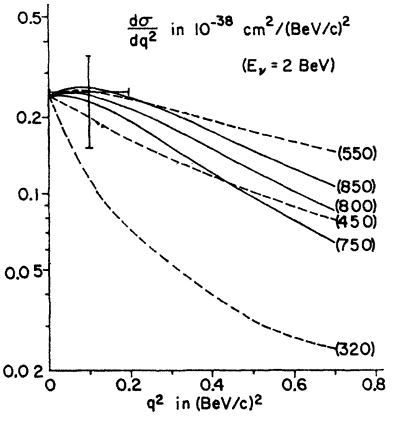

FIG. 10. Differential cross section for $\nu_\mu+n\to N^{*+}+\mu^-$ with $F_1^A(0)$, $F_1^V(0)$, and $F_2^V(0)$ derived from $SU(6)$ and the CVC hypothesis. Dashed curves refer to $n=1$, solid curves to $n=2$.

In order to determine individually the two vector form factors appearing in Eq. (5.10a), we now invoke the CVC hypothesis. The resulting linear relation, (2.12), then reduces to

$$(M_1+M_2)^2[F_1^V(0)+F_2^V(0)]+(M_2^2-M_1^2)F_3^V(0)=0 \quad (5.11)$$

at zero-momentum transfer. The N^* photoproduction analysis of Gourdin and Salin[21] indicates that the ratio $F_3^V(0)/F_2^V(0)$ is small. In addition, its effect in (5.11) is reduced by the appearance of a small coefficient. Hence from Eqs. (5.10a) and (5.11), we deduce that[14]

$$F_1^V(0)=-F_2^V(0)=3.75. \quad (5.12)$$

We now wish to argue that the effects of the remaining form factors are not appreciable. For this purpose, we make use of the results of Sec. IV, where the effectiveness of the individual form factors was investigated. The three form factors, F_3^V, F_4^V, and F_4^A can be safely eliminated since their contributions are found to be negligibly small. For the remaining form factors, F_2^A and F_3^A, the situation is not so clear. Static theory[25] leads one to believe that F_2^A itself is small, in which case its contribution to the cross sections will also be small. We shall assume this to be the case. For F_3^A, however, little can be said. Even though it has a doubly-induced nature, its contribution at $t=0$ is nonvanishing due to the N^*-N mass difference. Since there is no information on this term, we have dropped it.[26]

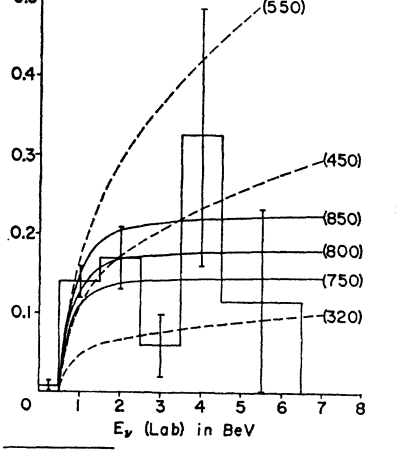

FIG. 11. Total cross section corresponding to Fig. 10.

For the three form factors now considered, we have plotted in Figs. 10 and 11 the N^{*+} production cross section for both the $n=1$ and $n=2$ cases for several values of b. The $SU(6)$ predictions are seen to be in reasonable accord with experiment[27,28] for the $n=2$ case with b close to the "elastic" value, $b=(850\text{ MeV})^2$. The $V-A$ interference term is constructive for this neutrino reaction. For the antineutrino process, the interference term is destructive and the corresponding curves have been plotted in Figs. 12 and 13. Further discussion will be presented in Sec. VI.

We now turn our attention briefly to the N-Y_1^* octet-decuplet transition. According to the $\Delta S/\Delta Q=+1$ rule, weak Y_1^* production from nucleons can only occur by antineutrinos according to

$$\bar{\nu}_\mu+p\to Y_1^{*0}+\mu^+, \quad (5.13)$$

and

$$\bar{\nu}_\mu+n\to Y_1^{*-}+\mu^+. \quad (5.14)$$

The production cross section for process (5.14) is twice that for (5.13); therefore, the cross section for Y_1^* production per nucleon is 1.5 times that for the Y_1^{*0} reaction.

The $SU(6)$ predictions are the following:

$$\frac{(p\tfrac{1}{2}\to Y_1^{*0}\tfrac{1}{2})_{V,\text{mag}}}{(p\tfrac{1}{2}\to N^{*0}\tfrac{1}{2})_{V,\text{mag}}}=\frac{1}{\sqrt{2}}\tan\theta, \quad (5.15a)$$

and

$$\frac{(p\tfrac{1}{2}\to Y_1^{*0}\tfrac{1}{2})_A}{(p\tfrac{1}{2}\to N^{*0}\tfrac{1}{2})_A}=\frac{1}{\sqrt{2}}\tan\theta. \quad (5.15b)$$

Taken together with the extended CVC hypothesis, the above then implies that

$$F_1^V(0)=-F_2^V(0)=2.85,\qquad F_1^A(0)=-0.59, \quad (5.16)$$

with $G=G_V\sin\theta$. We observe from Eqs. (5.15) that the Y_1^* and N^* antineutrino reactions are similar aside from

[25] See, e.g., J. S. Bell and S. M. Berman, Nuovo Cimento 25, 404 (1962).

[26] In Ref. 8, we allowed for a small deviation of F_2^A from zero. The relativistic $SU(6)$ theory predicts the normalizations of all eight form factors. It turns out that $F_2^A(0)$ is identically zero, while the contribution to the production cross section from F_3^A is relatively small. These results will be discussed elsewhere; see Ref. 9.

[27] The results presented in Figs. 10 and 11 differ slightly from those published earlier in Ref. 8. This is due to the choice of $\bar{M}=\frac{1}{2}(M_1+M_2)$ in Eq. (5.9) in place of M_1 as used previously.

[28] In the exact $SU(6)$ symmetry limit, only the direct axial-vector term, F_1^A, survives. In this limit, N. J. Papastamatiou and D. G. Sutherland [Phys. Letters 14, 246 (1965)] have also observed that the invariant differential cross section predicted by $SU(6)$ is compatible with the CERN experimental result (Ref. 5).

the $SU(3)$ coefficients, the tangent of the Cabibbo angle, and the mass effects.

We have assumed a Hofstadter-type q^2 dependence for F_1^V, F_2^V, and F_1^A and neglected all other form factor contributions, with somewhat less justification than previously. The ratio of Y^* to N^* production per nucleon is only about 1.5% and is plotted in Fig. 14 as a function of antineutrino energy.

VI. DISCUSSION OF THE RESULTS

Our purpose, as stated in the Introduction, has been to present a detailed phenomenological study of the neutrino-induced $N^*(1238)$ production process. To this end, we have invoked the local nature of the neutrino-lepton interaction to enable us to write the matrix element for this process in terms of eight form factors which are functions only of the momentum transfer

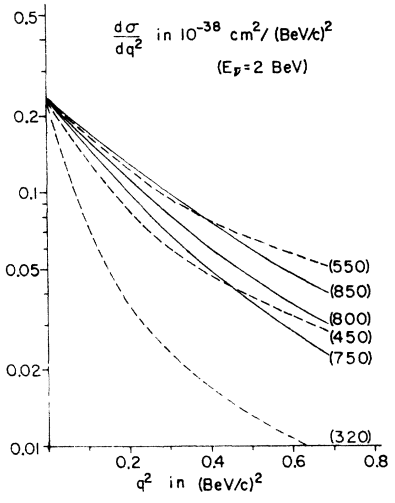

FIG. 12. Differential cross section for the antineutrino process, $\bar{\nu}_\mu + p \to N^{*0} + \mu^+$, with the same form factors employed as in Fig. 10.

variable. We have presented the general expression for the differential cross section for unpolarized weak N^* production in Appendix B. This formula is considerably more involved than its "elastic" counterpart, because of the higher intrinsic spin of the N^* isobar.

In Sec. IV, we have seen fit to limit our attention to the rather simple t-dependence of Eq. (4.1) for the form factors involved. As such, each form factor depends upon three parameters and, except for the structureless case, exhibits a singularity in the unphysical region for the production process. The three parameters are the normalization, $F_i^{V,A}(0)$; the order, n; and the location, $b_i^{V,A}$, of the pole in the complex t plane. In general, the analytic structure of these form factors is considerably more complicated; in effect, we have assumed that the structure of each one is dominated by an effective singularity on the real axis. This t dependence is not too unreasonable at low-momentum transfer and, in fact, for the "elastic" reaction, it fits the experimental results rather well. For practical purposes, we have

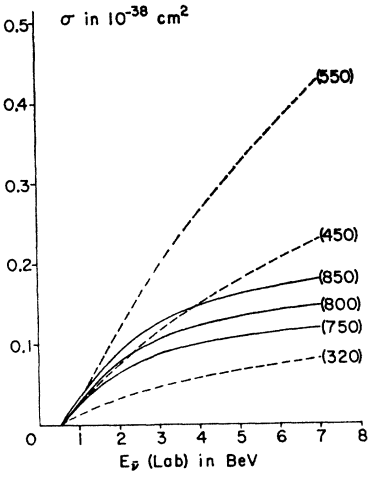

FIG. 13. Total cross section corresponding to Fig. 12.

assumed identical locations and orders of the effective poles for all eight form factors; in addition, we have confined our attention to three choices for n, i.e., $n=0$, 1, and 2, corresponding to a structureless, simple pole, and Hofstadter-type momentum transfer dependence.

Given this functional dependence for the form factors, one can make the following general remarks.[29] The invariant differential cross section at zero-momentum transfer depends solely on the normalizations of the form factors and is dominated by F_1^A. Cn the other hand, the asymptotic behavior of the total cross section for large s is a sensitive function of the parameter n as exhibited in Table II. This becomes apparent even at moderate neutrino energies as shown in Fig. 4. Consequently, we have dismissed the structureless case for which $\sigma(s)$ diverges at least quadratically with s and concentrated on the two cases, $n=1$ and 2. From threshold to 10-BeV neutrino energy, the first is characterized by a continuously rising cross section,

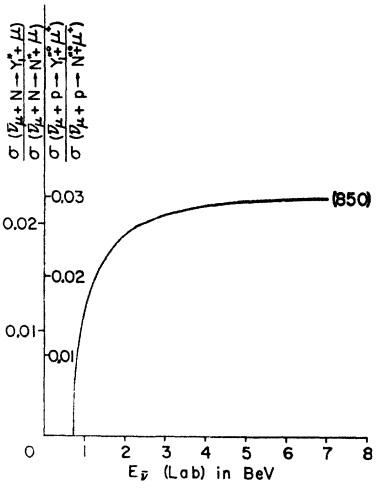

FIG. 14. Antineutrino cross section ratios for Y_1^* compared to N^* production. The form factors are determined from $SU(6)$ and the CVC hypothesis with $n=2$.

[29] These features were previously discussed in Ref. 7 for the $n=2$ case.

TABLE III. Form-factor parameters for the three models investigated. The characteristic values for $\sqrt{b}$ are drawn from the experimental results. Those in parentheses indicate that the fit is very poor.

Model	Form factor parameters $F_1^A(0)$	$F_1^V(0)$	$F_2^V(0)$	$(n=1)$ $\sqrt{b}$ (MeV)	$(n=2)$ $\sqrt{b}$ (MeV)
(1) Pure F_1^A	1.0	0	0	770	1220
(2) N^* photoproduction +CVC+F_1^A	−0.87	5.6	−5.6	(360)	670
(3) $SU(6)$+CVC	−0.83	3.75	−3.75	(450)	820

while the second leads to a cross section which saturates within this energy range. For fixed normalizations, $F_i^{V,A}(0)$, and given n, the shape of the differential cross section, and therefore the front-to-back ratio, depends critically upon the cutoff or "shape" parameter b. As b is increased, the total cross section increases while the F/B ratio decreases by orders of magnitude.

The effectiveness of each form factor in contributing to the cross sections has been investigated in some detail. This study is influenced to some extent by the mass one inserts to render all the form factors dimensionless. With the choice made in Sec. III and all form factors normalized to unity, we find that in the low-energy region they can be listed in decreasing order of effectiveness according to:

$$F_1^A,\ (F_1^V,F_2^V,F_2^A,F_3^A),\ F_3^V,\ F_4^A,\ F_4^V.$$

The ones within the parentheses are about equally effective.

We have attempted to derive some quantitative results from the current CERN experimental information on weak N^* production by considering several simple models. In each case, the $n=2$ Hofstadter-type form factors yield better results than the $n=1$ simple pole functions, since the experimental cross section appears to saturate within 8 BeV. Moreover, the information on $d\sigma/dt$ at low-momentum transfer suggests that F_1^A must be present to an appreciable amount: $F_1^A(0)\gtrsim 0.7$ with the same weak-coupling constant as in beta decay.

In Table III, we have recorded the form factor parameters characteristic of the three models considered. The first model is the simplest in that it singles out the importance of F_1^A alone. In the second model, $F_1^V(0)$ and $F_2^V(0)$ are determined uniquely from the work of Gourdin and Salin on N^* photoproduction, while $F_1^A(0)$ is adjusted to yield the observed differential cross section. On the other hand, all three form factors at zero-momentum transfer are determined by $SU(6)$ and the CVC hypothesis.

The predictions of the $SU(6)$ symmetry scheme are obviously of greatest interest. This scheme appears to triumph on three counts. First, the prediction for the magnitude of $F_1^A(0)$ is just what is required to give the correct differential cross section at low-momentum transfer. Second, the V-A interference effect is constructive and large in agreement with the rapidly rising N^* production cross section just above threshold. And third, the Hofstadter-type cutoff parameter is characteristic of that for the elastic reaction, $b\approx(850\text{ MeV})^2$. These predictions are rather remarkable—and perhaps somewhat fortuitous.

It is somewhat curious that the predictions from the N^* photoproduction data do not yield better results. With $b=(850\text{ MeV})^2$ and $n=2$, the total cross section prediction is much too large.[30] Only with a considerably smaller value of $(670\text{ MeV})^2$ is reasonable agreement obtained.

On the basis of $SU(6)$, N^* production by antineutrinos is suppressed at low energies by the large destructive V-A interference effect. This is also typical of the elastic reaction. Y_1^* production by antineutrinos is suppressed also by the Cabibbo angle and unfavorable $SU(3)$ Clebsch-Gordan coefficients. These predictions serve as a test for this model.

We shall extend our analysis elsewhere[9] to include the predictions of the relativistic generalizations of the $SU(6)$ theory.[31]

ACKNOWLEDGMENTS

We thank with pleasure Professor M. M. Block for stimulating our interest in neutrino reactions and for many valuable discussions. We also wish to thank Professor L. M. Brown for his continued interest in this work.

APPENDIX A: KINEMATICS

1. Center-of-Mass System (c.m.s.)

In the c.m.s. of the s channel, we define

$$\begin{aligned} k_1&=(\mathbf{k}_1,i\omega_1), \quad & k_2&=(\mathbf{k}_2,i\omega_2),\\ p_1&=(-\mathbf{k}_1,iE_1), \quad & p_2&=(-\mathbf{k}_2,iE_2). \end{aligned} \tag{A1}$$

The two independent scalar variables are

$$s=W^2, \quad t=m_l^2-2\omega_1\omega_2+2\omega_1|\mathbf{k}_2|\cos\theta, \tag{A2}$$

where W is the total c.m. energy and θ is the c.m. angle between the outgoing lepton and the incident neutrino.

[30] This point was also observed by Berman and Veltman, see Ref. 10.

[31] *Note added in proof.* After submission of our manuscript, it has come to our attention that members of the CERN heavy-liquid bubble-chamber group have recently made a more detailed analysis of single pion production in neutrino reactions than that published in Ref. 5. Since the new experimental cross section is considerably larger than the published one, the predictions of the $SU(6)$ theory now appear to be less favorable. A summary of the results obtained in this paper with reference to both the published and the new experimental findings is presented in Ref. 9.

We wish to thank Professor Ph. Salin and Professor C. Franzinetti for informing us of the new results prior to publication.

The momenta and energies in the c.m.s. are

$$2W|\mathbf{k}_1| = s-M_1^2,$$
$$2W|\mathbf{k}_2| = \{[s-(M_2-m_l)^2][s-(M_2+m_l)^2]\}^{\frac{1}{2}}; \quad \text{(A3)}$$

$$\omega_1 = |\mathbf{k}_1|, \quad 2W\omega_2 = s-M_2^2+m_l^2,$$
$$2WE_1 = s+M_1^2, \quad 2WE_2 = s+M_2^2-m_l^2. \quad \text{(A4)}$$

The differential cross section in the c.m.s. for N^* production is given by

$$\frac{d\sigma}{d\cos\theta} = 2\omega_1|\mathbf{k}_2|\frac{d\sigma}{dt}, \quad \text{(A5)}$$

where $d\sigma/dt$ is given by Eq. (3.1).

2. Laboratory System

In the lab where the target nucleon is at rest, we define

$$k_1 = (\mathbf{k}_1, i\omega_1), \quad k_2 = (\mathbf{k}_2, i\omega_2),$$
$$p_1 = (0, iM_1), \quad p_2 = (\mathbf{p}_2, iE_2). \quad \text{(A6)}$$

Here

$$s = M_1^2+2\omega_1 M_1, \quad t = m_l^2-2\omega_1\omega_2+2\omega_1|\mathbf{k}_2|\cos\theta_l, \quad \text{(A7)}$$

where θ_l is the lab angle between the outgoing lepton and the incident neutrino. The momenta and energies are now given by

$$2M_1|\mathbf{k}_1| = s-M_1^2,$$
$$2M_1|\mathbf{k}_2| = \{[s+t-M_2^2-2M_1m_l] \times [s+t-M_2^2+2M_1m_l]\}^{\frac{1}{2}},$$
$$2M_1|\mathbf{p}_2| = \{[(M_1+M_2)^2-t][(M_1-M_2)^2-t]\}^{\frac{1}{2}}; \quad \text{(A8)}$$

$$\omega_1 = |\mathbf{k}_1|, \quad 2M_1\omega_2 = s+t-M_2^2,$$
$$2M_1E_2 = M_1^2+M_2^2-t. \quad \text{(A9)}$$

Let θ^* be the angle between the N^* isobar and the incident neutrino. The maximum laboratory angle, $\theta_{\max}^*$, is determined by

$$\sin\theta_{\max}^* = M_1\{[s-(M_2+m_l)^2] \times [s-(M_2-m_l)^2]\}^{\frac{1}{2}}/[M_2(s-M_1^2)]. \quad \text{(A10)}$$

The differential cross sections in the lab are related to the invariant differential cross section according to

$$\frac{d\sigma}{d\cos\theta} = \frac{2\omega_1 M_1|\mathbf{k}_2|^2}{(M_1+\omega_1)|\mathbf{k}_2|-\omega_1\omega_2\cos\theta}\frac{d\sigma}{dt},$$
$$\frac{d\sigma}{d\cos\theta^*} = \frac{2\omega_1 M_1|\mathbf{p}_2|^2}{\omega_1 E_2\cos\theta^*-|\mathbf{p}_2|(M_1+\omega_1)}\frac{d\sigma}{dt}. \quad \text{(A11)}$$

APPENDIX B: INVARIANT DIFFERENTIAL CROSS SECTION

The invariant differential cross section is given by Eq. (3.1) as

$$\frac{d\sigma}{dt} = \frac{1}{2\pi}\frac{T}{(s-M_1^2)^2}, \quad \text{(B1)}$$

where

$$T = \tfrac{4}{3}G^2\sum_{i=1}^{5}R_i(t)X_i(s,t). \quad \text{(B2)}$$

The functions $X_i(s,t)$ of Eq. (3.7) are given explicitly in terms of s and t according to

$$4X_1 = (s-M_1^2)(s-M_2^2-m_l^2) + (s+t-M_1^2-m_l^2)(s+t-M_2^2), \quad \text{(B3a)}$$
$$4X_2 = (s-M_1^2)(s-M_2^2-m_l^2) - (s+t-M_1^2-m_l^2)(s+t-M_2^2), \quad \text{(B3b)}$$
$$4X_3 = (s-M_2^2-m_l^2)(s+t-M_1^2-m_l^2), \quad \text{(B3c)}$$
$$4X_4 = (s-M_1^2)(s+t-M_2^2), \quad \text{(B3d)}$$
$$2X_5 = M_1M_2(t-m_l^2). \quad \text{(B3e)}$$

The functions $R_i(t)$ are found to be

$$R_1 = r^2uv(|F_2^A|^2+|F_2^V|^2)+r\,\mathrm{Re}(F_1^AF_2^{A*}-F_1^VF_2^{V*}) - r^4uv(M_2/M_1)[u(|F_3^A|^2-|F_4^A|^2)+v(|F_3^V|^2-|F_4^V|^2)] - r^2((t-M_1^2+M_2^2)/2M_1M_2)\,\mathrm{Re}(uF_1^AF_3^{A*}+vF_1^VF_3^{V*}) - r^2((t-M_1^2-3M_2^2)/2M_1M_2)\,\mathrm{Re}(uF_1^AF_4^{A*}+vF_1^VF_4^{V*}) + r^2uv\,\mathrm{Re}[F_2^AF_3^{A*}-F_2^VF_4^{V*}+((M_2-M_1)/(M_1+M_2))(F_2^VF_3^{V*}-F_2^AF_4^{A*})], \quad \text{(B4a)}$$

$$R_2 = -\mathrm{Re}(F_1^AF_1^{V*}+ruF_1^AF_2^{V*}+rvF_1^VF_2^{A*}-2r^2uvF_2^AF_2^{V*}), \quad \text{(B4b)}$$

$$R_3 = -(M_1/M_2)(u|F_1^A|^2+v|F_1^V|^2)-r(M_1/M_2)\,\mathrm{Re}(F_1^AF_2^{A*}+F_1^VF_2^{V*}) - r^4uv(M_2/M_1)[u(|F_3^A|^2+|F_4^A|^2)+v(|F_3^V|^2+|F_4^V|^2)]+r((t-M_1^2-M_2^2)/M_2^2) \times\mathrm{Re}[F_1^AF_2^{A*}-F_1^VF_2^{V*}-ru(M_2/M_1)F_1^A(F_3^{A*}-F_4^{A*})-rv(M_2/M_1)F_1^V(F_3^{V*}-F_4^{V*})] + 2r^3uv\,\mathrm{Re}[F_2^A(F_3^{A*}-F_4^{A*})-F_2^V(F_3^{V*}-F_4^{V*})]+2r^4uv(M_2/M_1)\,\mathrm{Re}(uF_3^AF_4^{A*}+vF_3^VF_4^{V*}), \quad \text{(B4c)}$$

$$R_4 = -r^4uv(M_2/M_1)(u|F_3^A+F_4^A|^2+v|F_3^V+F_4^V|^2)+r(M_2/M_1)\,\mathrm{Re}(F_1^AF_2^{A*}+F_1^VF_2^{V*}) - 2r^2(M_2/M_1)\,\mathrm{Re}[uF_1^A(F_3^{A*}+F_4^{A*})+vF_1^V(F_3^{V*}+F_4^{V*})] + 2r^3uv(M_2/M_1)\,\mathrm{Re}[F_2^A(F_3^{A*}+F_4^{A*})+F_2^V(F_3^{V*}+F_4^{V*})], \quad \text{(B4d)}$$

$$R_5=\tfrac{1}{2}(u|F_1{}^A|^2+v|F_1{}^V|^2)+r^2uv(|F_2{}^A|^2-|F_2{}^V|^2)+r^4uv((t-2M_1{}^2-2M_2{}^2)/2M_1{}^2)(u|F_3{}^A|^2+v|F_3{}^V|^2)$$
$$-r^4uv(t/2M_1{}^2)(u|F_4{}^A|^2+v|F_4{}^V|^2)-ruv\,\mathrm{Re}(F_1{}^AF_2{}^{A*}+F_1{}^VF_2{}^{V*})$$
$$+r^2uv\,\mathrm{Re}[u(F_1{}^AF_3{}^{A*}+F_1{}^AF_4{}^{A*}-F_2{}^AF_3{}^{A*})+v(F_1{}^VF_3{}^{V*}+F_1{}^VF_4{}^{V*}+F_2{}^VF_4{}^{V*})]$$
$$+r^2uv((M_2-M_1)/(M_1+M_2))[u(F_2{}^AF_4{}^{A*}+F_3{}^AF_4{}^{A*})-v(F_2{}^VF_3{}^{V*}-F_3{}^VF_4{}^{V*})], \quad \text{(B4e)}$$

where

$$r=M_1/(M_1+M_2), \quad 2M_1M_2u=t-(M_1+M_2)^2, \quad 2M_1M_2v=t-(M_1-M_2)^2. \quad \text{(B5)}$$

APPENDIX C: TOTAL CROSS SECTION

As stated in Sec. IV, we have adopted the following phenomenological t dependence for the form factors:

$$F_i{}^{V,A}(t)=\frac{F_i{}^{V,A}(0)}{(1-t/b)^n}. \quad \text{(C1)}$$

For the two cases of interest, $n=1$ and $n=2$, the invariant differential cross section of Eq. (B1) may be integrated analytically to yield the following results:

$$\sigma(s)=\frac{G^2}{4\pi}\frac{b^2}{(s-M_1{}^2)^2}\frac{2}{3}\int_{t_{\min}}^{t_{\max}}h^{(1)}(s,t)dt, \quad \text{for } n=1,$$
$$\sigma(s)=\frac{G^2}{4\pi}\frac{b^4}{(s-M_1{}^2)^2}\frac{2}{3}\int_{t_{\min}}^{t_{\max}}h^{(2)}(s,t)dt, \quad \text{for } n=2, \quad \text{(C2)}$$

where

$$t_{\min}=M_1{}^2+M_2{}^2-2E_2E_1-2|\mathbf{p}_2||\mathbf{p}_1|, \quad t_{\max}=M_1{}^2+M_2{}^2-2E_2E_1+2|\mathbf{p}_2||\mathbf{p}_1|. \quad \text{(C3)}$$

The momenta and energies appearing in (C3) refer to the center-of-mass variables defined in Appendix A1 and are functions only of s.

The indefinite integrals of $h^{(n)}(s,t)$ are tabulated below. Terms involving $F_4{}^V$ and $F_4{}^A$ have been dropped, since they yield extremely small contributions to the N^* production process.

$$\int h^{(n)}(s,t)dt=\sum_{i=1}^{16}S_i{}^{(n)}(s,t); \quad n=1,2 \quad \text{(C4)}$$

$$S_1{}^{(n)}=-|F_1{}^A(0)|^2[d_1I_n(u)+d_2I_n(ut)],$$

$$S_2{}^{(n)}=-|F_1{}^V(0)|^2[d_1I_n(v)+d_2I_n(vt)],$$

$$S_3{}^{(n)}=r^2|F_2{}^A(0)|^2[(d_3-2M_1M_2m_l{}^2)I_n(uv)+(d_4+2M_1M_2)I_n(uvt)+I_n(uvt^2)],$$

$$S_4{}^{(n)}=r^2|F_2{}^V(0)|^2[(d_3+2M_1M_2m_l{}^2)I_n(uv)+(d_4-2M_1M_2)I_n(uvt)+I_n(uvt^2)],$$

$$S_5{}^{(n)}=2r^2|F_3{}^A(0)|^2\{((M_1/M_2)d_5-m_l{}^2d_6)I_n(uv)$$
$$-[(r^2/M_1M_2)d_5-(1+(m_l{}^2r^2/M_1{}^2))d_6]I_n(uvt)-(r^2/M_1{}^2)d_6I_n(uvt^2)\},$$

$$S_6{}^{(n)}=2r^2|F_3{}^V(0)|^2\Big\{((M_2-M_1)/(M_1+M_2))^2((M_1/M_2)d_5-m_l{}^2d_6)I_n(uv)$$
$$-\left[\frac{r^2}{M_1M_2}d_5-\frac{(M_2-M_1)^2+m_l{}^2}{(M_1+M_2)^2}d_6\right]I_n(uvt)-\frac{r^2}{M_1{}^2}d_6I_n(uvt^2)\Big\},$$

$$S_7{}^{(n)}=r\,\mathrm{Re}[F_1{}^A(0)F_2{}^{A*}(0)][(d_1+d_3+d_5-M_1M_2m_l{}^2)I_n(1)+(d_2+d_4+sM_2/M_1)I_n(t)$$
$$+I_n(t^2)+2(d_1-M_1M_2m_l{}^2)I_n(u)+2(d_2+M_1M_2)I_n(ut)+2M_1M_2m_l{}^2I_n(uv)-2M_1M_2I_n(uvt)],$$

$$S_8{}^{(n)}=r\,\mathrm{Re}[F_1{}^V(0)F_2{}^{V*}(0)][(d_1-d_3+d_5-M_1M_2m_l{}^2)I_n(1)+(d_2-d_4+sM_2/M_1)I_n(t)$$
$$-I_n(t^2)-2(d_1-M_1M_2m_l{}^2)I_n(v)-2(d_2+M_1M_2)I_n(vt)+2M_1M_2m_l{}^2I_n(uv)-2M_1M_2I_n(uvt)],$$

$$S_9^{(n)}=-r\,\mathrm{Re}[F_1^A(0)F_3^{A*}(0)]\{[((M_2-M_1)/(M_1+M_2))(2d_3+m_l^4)+m_l^2d_4]I_n(u)$$
$$+[2((M_2-M_1)/(M_1+M_2))d_4+M_2^2-M_1^2+m_l^2]I_n(ut)+((M_2-M_1)/(M_1+M_2))I_n(ut^2)$$
$$+2r[d_3-m_l^2(s+M_1M_2-m_l^2)]I_n(uv)+2r[d_4+M_1(M_1+M_2)]I_n(uvt)\},$$

$$S_{10}^{(n)}=-r\,\mathrm{Re}[F_1^V(0)F_3^{V*}(0)]\{[2d_3+m_l^4+((M_2-M_1)/(M_1+M_2))m_l^2d_4]I_n(v)$$
$$+[2d_4+((M_2-M_1)/(M_1+M_2))(M_2^2-M_1^2+m_l^2)]I_n(vt)+I_n(vt^2)$$
$$+2r[d_3-m_l^2(s-M_1M_2-m_l^2)]I_n(uv)+2r[d_4+M_1(M_1-M_2)]I_n(uvt)\},$$

$$S_{11}^{(n)}=2r^2\,\mathrm{Re}[F_2^A(0)F_3^{A*}(0)]\{[r(d_3+2d_5+m_l^4)-m_l^2(s+M_1M_2)]I_n(uv)+(2s-rm_l^2)I_n(uvt)\},$$

$$S_{12}^{(n)}=-2r^2\,\mathrm{Re}[F_2^V(0)F_3^{V*}(0)]\{[r(d_3-2d_5+m_l^4)+((M_2-M_1)/(M_1+M_2))m_l^2(s-M_1M_2)]I_n(uv)$$
$$-[2((M_2-M_1)/(M_1+M_2))s+rm_l^2]I_n(uvt)\},$$

$$S_{13}^{(n)}=\mathrm{Re}[F_1^A(0)F_1^{V*}(0)][(M_2^2-M_1^2)m_l^2I_n(1)+d_4I_n(t)+I_n(t^2)],$$

$$S_{14}^{(n)}=r\,\mathrm{Re}[F_1^A(0)F_2^{V*}(0)][(M_2^2-M_1^2)m_l^2I_n(u)+d_4I_n(ut)+I_n(ut^2)],$$

$$S_{15}^{(n)}=r\,\mathrm{Re}[F_2^A(0)F_1^{V*}(0)][(M_2^2-M_1^2)m_l^2I_n(v)+d_4I_n(vt)+I_n(vt^2)],$$

$$S_{16}^{(n)}=-2r^2\,\mathrm{Re}[F_2^A(0)F_2^{V*}(0)][(M_2^2-M_1^2)m_l^2I_n(uv)+d_4I_n(uvt)+I_n(uvt^2)].$$

We have condensed the above expressions by using the following formulas:

$$d_1=[(s-M_1^2-m_l^2)(s-M_2^2-m_l^2)+M_2^2m_l^2]M_1/M_2, \qquad d_4=2s-M_1^2-M_2^2-m_l^2,$$
$$d_2=(s-2M_2^2-m_l^2)M_1/M_2, \qquad d_5=(s-M_1^2)(s-M_2^2)M_2/M_1, \tag{C5}$$
$$d_3=2s^2-2s(M_1^2+M_2^2+m_l^2)+2M_1^2M_2^2+m_l^2(M_1^2+M_2^2), \qquad d_6=s-m_l^2/4,$$

and

$$I_n(y)=\int\frac{ydt}{(t-b)^{2n}}. \tag{C6}$$

The symbols r, u, and v were previously defined in Appendix B.

In the above formulas, we have adopted a universal cutoff parameter for all eight form factors, i.e., $b_i^{V,A}=b$, for simplicity. If this restriction is relaxed, the changes that must be made in Eqs. (C2), (C4), and (C6) are both trivial and obvious.